International Journal for Housing Science and Its Applications
Publish August 6, 2025. Volume 46, Issue 3 Pages 7403-7416

https://doi.org/10.70517/ijhsa463635

Characterization of PBDE and new brominated flame retardants contamination in copper laminate sorting residues based on machine learning algorithms

Yanzhi Chen[1,2,*], Hong Deng[1], Guangfu Hua[2] and Wei Wang[2]
[1] School of Environment and Energy, South China University of Technology, Guangzhou Higher Education Mega Centre, Guangzhou, Guangdong, 510006, China
[2] South China Institute of Environmental Sciences, Guangzhou, Guangdong, 510655, China
Corresponding authors: (e-mail: cyz798798@163.com).

Abstract Polybrominated diphenyl ethers (PBDEs) and novel brominated flame retardants (NBFRs) are widely used as important flame retardants in electronic products such as copper laminates. In this study, a simple Bayesian model combined with the XGBoost algorithm was used to analyze the contamination characteristics of PBDEs (polybrominated diphenyl ethers) and NBFRs (novel brominated flame retardants) in the sorting residues of copper laminates. GC/MSD was applied to detect and analyze the residues from nine sampling sites. The results showed that BDE99 was detected at all monitoring sites with a detection frequency of 100%, and its concentration ranged from 0.158 to 0.498 ng/L, with the highest concentration of 1.657 ng/L at site H1. Among the eight PBDEs monomers detected, the detection rate of BDE47, BDE99, BDE100, and BDE209 was 100%, and the Σ7PBDEs the contents ranged from 9.166~88.326ng·g-1, and the median value was 29.092ng·g-1. Among the novel brominated flame retardants, the detection rate of BPA was 84.648%, and the detection rates of BPB and BPAF were both 61.548%. Correlation analysis showed that there was a significant positive correlation between BPA and BPAF ($r=0.54$, $p=0.048<0.05$). The time trend analysis showed that the ratio of Σ26PBDEs/Σ5NBFRs showed a decreasing trend from 4.233 in 2011 to 2.073 in 2021, which indicated that the new brominated flame retardants were gradually replacing the traditional PBDEs.The machine-learning based analysis method effectively identified the main controlling factors of the contamination characteristics, and provided scientific basis for the management of the contaminated sites and the control of risks.

Index Terms Polybrominated diphenyl ethers (PBDEs), Novel brominated flame retardants, Machine learning, XGBoost, Simple Bayes, Pollution characterization

I. Introduction

Printed circuit board (PCB) is the most active industry in contemporary electronic components, according to the survey in 2003 China's production value of printed circuit boards has exceeded the United States, second to Japan, ranking second in the world. Although the PCB industry is not included in the heavy pollution industry, it deserves our attention as a relative water and energy consumption, and at the same time, it is an industry with more pollutant discharges [1], [2]. The pollution of PCB manufacturing enterprises is mainly generated in the drilling, etching, plating, metallization, de-filming, developing and other processes, and the pollutants discharged are mainly industrial wastewater, followed by solid wastes [3]-[5]. However, previous studies have paid more attention to the pollution problem of heavy metals in wastewater and fixed waste, and less attention to the pollution problem in the drilling and etching process [6].

Glass fibers and other reinforcing materials through the bonding material crosslinked to form a bonding sheet, and then in the laminating machine will be bonded sheet and copper box according to the design requirements of the laminated up, the bonding sheet and the copper box layer is firmly bonded into the substrate, and then in the substrate through the light candle engraving or chemical copper precipitation process to form a PCB circuit board. In the above copper lamination process produces a variety of waste categories, a wide range of pollutants [7]. Among them, bromine-based flame retardants, which are widely used in PCB products to ensure their fire rating, have the potential to migrate these residual substances from PCB products, causing environmental pollution [8]-[11]. Although in the large-scale, full-fledged facilities of the production enterprises, each production plant has the appropriate waste collection devices and treatment, such as etching solution, plating solution and other high-concentration waste liquids are categorized and collected in containers, and then entrusted to a company with the treatment of subsidies for the treatment of high-concentration waste liquids [12]-[14]. However, it is necessary to manage and categorize the physicochemical properties of these pollutants as well as the pollution

characteristics, so as to develop targeted pollution prevention and control means to contribute to the ecological environment management [15].

Brominated flame retardants (BFRs) in e-waste have become an environmental pollutant of global concern, especially the environmental risks caused by polybrominated diphenyl ethers (PBDEs) and new brominated flame retardants (NBFRs) in copper laminate sorting residues are becoming increasingly prominent. Epoxy resin-based copper-clad laminates, which account for a significant proportion of PCB materials, are widely used due to their excellent adhesion, electrical insulation and low-cost characteristics. However, epoxy resins are poor in heat and moisture absorption resistance, and need to be improved by the addition of flame retardants, which are released into the environment at the end of the product's life cycle. The use of resin matrix materials such as polyimide (PI), bismaleimide (BMI), cyanate ester resin (CE) and polyphenylene ether (PPE) has further increased the diversity of flame retardants, of which TBBPA, the largest brominated flame retardant in terms of production volume, with an annual production volume of about 120,000 tons, is mainly used for flame retardancy of printed wiring boards, but studies have confirmed that it releases TBBPA and its metabolites into the environment. The hot pressing process and the dip-drying step in the preparation of copper laminates affect the distribution and release of flame retardants, and the residues generated during the sorting process become important carriers of these contaminants. Traditional contamination characterization methods are often difficult to comprehensively identify the distribution patterns and interrelationships of multiple contaminants in complex matrices, especially in the face of the lack of effective means of downscaling and feature selection for high-dimensional feature data. Machine learning algorithms provide a new way to solve this problem, with the simple Bayesian model able to classify samples based on prior knowledge, and the XGBoost algorithm able to efficiently process high-dimensional data and calculate feature importance. By associating these two methods, a comprehensive analysis framework that can both classify and quantify pollution features can be constructed, which not only identifies the main controlling factors of pollution severity, but also quantifies the contribution of each feature to the pollution level through weight calculation. In this study, we combine the plain Bayes and XGBoost algorithms to construct a machine-learning-based pollution feature mining method to systematically analyze PBDEs and NBFRs in copper laminate sorting residues, assess the spatial distribution characteristics, concentration levels and substitution trends of the pollutants, and identify the key factors affecting the pollution degree, so as to provide scientific basis for the precise management and risk control of the contaminated sites. At the same time, it provides new technical means for the study of environmental behavior of brominated flame retardants in e-waste.

II. Preparation of copper laminates

II. A. Structural characteristics and development of copper-clad laminates

II. A. 1) Resin matrix

Epoxy resin-based copper-cladding board in the PCB material occupies a considerable proportion, is also widely used in a matrix resin. This is mainly due to the epoxy resin has excellent adhesion, electrical insulation, excellent processability, easy modification and low cost and other characteristics. However, epoxy resin heat resistance, moisture absorption resistance is poor, can not adapt to the use of high-frequency high-performance PCB requirements, so it is necessary to carry out reasonable modification of epoxy resin.

II. A. 2) Polyimide (PI) and bismaleimide (BMI)

Polyimide resin (PI) has excellent dielectric, mechanical, radiation, corrosion, ablation and other properties, mainly due to the molecular main chain contains imide ring structure.PI is usually used as a flexible printed circuit boards, the peel strength is high, mainly due to the linear coefficient of expansion of the polyphthalimide and copper foil similar to that caused by the PI resin, although it has excellent performance, but the thermal expansion coefficient of the PI copper cladding board is much larger than the thermal expansion coefficient of electronic components, when used in circuits, due to the presence of internal stress in the product, cracks often occur, and even fracture, when applied in the circuit, due to the presence of internal stress in the product, often resulting in cracks, and even fracture, the thermal expansion coefficient of electronic components. Although PI resin has excellent performance, the coefficient of thermal expansion of PI laminate is much larger than that of electronic components, when applied to the circuit, due to the existence of internal stress in the product, cracking phenomenon often occurs, and even fracture, which seriously affects the performance of PI copper-clad laminates. Therefore, in order to broaden its application in the copper cladding industry, PI resin must be modified.

II. A. 3) Cyanate ester resins (CE)

CE resin has good dielectric properties and heat resistance, and began to be widely used in the 1980s. In fact, as early as the 1950s, some simple cyanate ester compounds were synthesized, but due to the constraints of the conditions at that time, the yields and purity of the products obtained were low, thus limiting their further

development. In 1976, Bayer of West Germany produced the first commercialized cyanate ester resin, known as triazine. At that time, it was only used as a substitute for polyimide high-temperature-resistant resins, although the resin also has good electrical properties, but due to high moisture absorption, poor chemical resistance, poor compatibility and other reasons, and ultimately withdrawn from the market in 1987. However, in the following year, Mitsubishi Gas Chemical Corporation of Japan developed and synthesized bismaleimide triazine resin (referred to as BT resin) by utilizing Bayer's technology. BT resin combines the excellent properties of BMI and CE resins with heat resistance, low dielectricity, and good mechanical properties and dimensional stability. At present, Mitsubishi Gas has been occupying this market. In the 1980s, various types of cyanate ester resins were developed and widely used.

II. A. 4) Polyphenylene ether (PPE)

Polyphenylene ethers are generally synthesized by two methods, one is obtained by oxidative coupling reaction of 2,6-dimethylphenol [16]. The other is 2,6-dimethyl phenol etherification reaction polycondensation, polyphenylene ether resin has a low dielectric constant and low loss factor (er for 2.45, tand 0.0007), high glass transition temperature, dimensional stability, good and high mechanical strength, low water absorption (water absorption of 0.05%), acid, alkali, salt resistance is good, there are good self-extinguishing, a little treatment can be up to UL94-V0 grade, etc., due to the PPE resin heat resistance, heat resistance of the PPE resin can be obtained. V0 level and other advantages, due to the low heat resistance of PPE resin can not be directly applied to PCB substrate.

II. B.Copper laminate material preparation

II. B. 1) Main raw materials

(1) Resin base

PPESK (S/K=1:1, characteristic viscosity 0.42dL/g), PPENK (N/K=1:1, characteristic viscosity 0.43dL/g) are supplied by Dalian Baolimo New Material Co.

During the production process of the resin, it is often accompanied by the presence of some metal ions (Nat, Cat, Mg2t, Fe3t, Fe2t), which have a great influence on the dielectric properties of the resin, as well as on the thermal and mechanical properties of the material [17]. Therefore, it is necessary to purify the resin to remove the metal ions in the system in order to achieve the best use. The polymer was dissolved in chloroform, filtered and precipitated in ethanol, filtered, dried and then boiled (1% water containing HCl), and replaced with deionized water for 5 times until the pH reaches 7, filtered, dried and set aside.

(2) Copper foil and surface treatment

The viscosity of silane coupling agent is small, low surface tension, can be impregnated in the very small gaps on the surface of the object to be adhered. On the other hand, it can produce mutual coupling effect with the surface of the adherend, and thus can effectively improve the bonding strength. Analysis of the chemical structure of silane coupling agent shows that it can form chemical bonds with inorganic materials, metal surfaces and organic resins respectively, which effectively improves the bonding strength of the interface layer. According to these characteristics of silane coupling agent, it is often used in the bonding process. Surface treatment of copper foil: add the silane coupling agent to the resin glue, the dosage is 0.5-2% of the resin content (mass ratio), coated on the surface of clean metal copper foil, dry, standby.

II. B. 2) Preparation of copper-clad laminates

(1) Preparation of resin glue

Resin glue preparation quality directly affects the quality of the dip glue, in which the resin glue concentration is the key. Resin glue concentration has two effects, one is to affect the fiber wettability, and the other is to affect the amount of adhesive bonding piece of glue. If the concentration of resin glue is big, the viscosity will be big and the wetting of fiber will be poor, if the concentration of resin glue is small, the viscosity will be small, which will lead to the insufficient hanging quantity of bonding sheet. Usually, the type of resin, molecular weight, concentration and temperature affect the viscosity of resin glue.

Preparation: The polymer used is dissolved in a specific solvent or a mixture of solvents according to its intrinsic properties, stirring is used to accelerate its dissolution, and after the solution is formed into a homogeneous state, the stirring is stopped and it is sealed for backup.

(2) Soak and dry

Using a single solvent to formulate the glue, in the removal of solvents will leave a large number of holes in the bonded piece of the surface and the interior, ultimately resulting in a decline in the performance of the finished product. In order to avoid these defects of a single solvent, this paper applies a mixture of solvents to dissolve the resin, step by step temperature method to remove the solvent.

The high performance thermoplastic resin used in this experiment has a large molecular weight and is easy to form a film, so the temperature in the drying process can not be raised too quickly, if it is raised too quickly, it is easy to form a large number of bubbles on the surface, which ultimately affects the mechanical properties of the laminate.

(3) Hot pressing process

Copper laminates are generally prepared by hot pressing. The so-called hot pressing method is at a certain temperature and pressure, the dip material bonding sheet melting molding, and then cooling solidification, demolding, to get the required copper-clad laminate. Copper-clad laminate hot pressing schematic shown in Figure 1 [18].

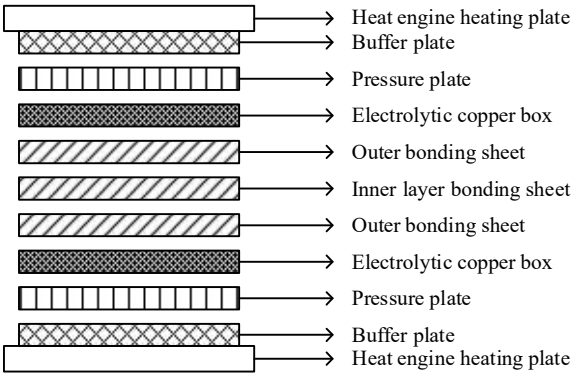

Figure 1: Hot-pressing diagram of Copper Clad Laminate

III. PBDEs and new brominated flame retardants in copper laminate residues

III. A. Machine learning-based feature mining for residue contamination

III. A. 1) Research methodology

In accordance with the classification indicators of the Technical Provisions on Risk Screening and Risk Grading of Closed and Relocated Enterprise Sites [hereinafter referred to as “the Provisions”], the sampling data were divided into characteristic datasets, in which the main characteristics include the concentration of each type of pollutant exceeding the multiple times of the standard, the surface cover, the underground seepage control measures, the texture of the soil, the mode of land use, and the average sampling depth. Referring to the quantitative indicators in the Regulations, the pollutant characterization dataset was divided into two categories of medium concern and high concern according to the pollution severity. A Bayesian model was established to assess the probability of each sample belonging to high concern and medium concern, respectively. Figure 2 shows the technical route, using the XGBoost algorithm, calculating the feature importance of each feature, identifying the main control features of pollution severity, and using this quantification result as the weight to quantify the value of pollution features of each sample. Based on the ARCGIS platform, the pollution distribution map of the plant area is drawn to analyze the characteristics of pollutant distribution within the plant area, which provides a scientific reference for the management, remediation and control decision-making of the polluted site.

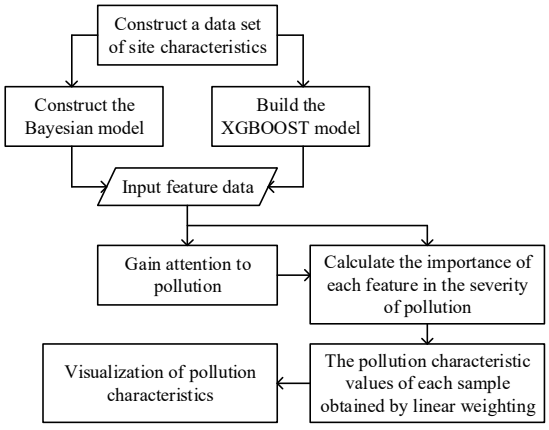

Figure 2: Technical research route

III. A. 2) Plain Bayesian modeling

Plain Bayes is a model in Bayesian classifiers, training the model with data sets of known categories, so as to realize the category judgment of unknown category data, the theoretical basis is Bayesian decision theory, the core idea is to use the prior knowledge to calculate the probability of samples belonging to each category respectively, as a way to determine the category to which the sample belongs to, so it is necessary to introduce the Bayesian probability formula for calculating the sample probability [19].

The Bayesian formula is generally expressed as:

$$P(B \mid A) = \frac{P(A \mid B)}{P(A)} * P(B) \tag{1}$$

It can also be loosely expressed as:

$$P(\text{Category} \mid \text{Features}) = \frac{P(\text{Features} \mid \text{Category})}{P(\text{Features})} * P(\text{Category}) \tag{2}$$

Assuming that a set of samples needs to be categorized into two categories, it is only necessary to calculate the probability that each sample belongs to category 1 and category 2, respectively, as shown in the following equation:

$$P(\text{Category 1} \mid \text{Features}) = \frac{P(\text{Features} \mid \text{Category 1})}{P(\text{Features})} * P(\text{Category 1}) \tag{3}$$

$$P(\text{Category 2} \mid \text{Features}) = \frac{P(\text{Features} \mid \text{Category 2})}{P(\text{Features})} * P(\text{Category 2}) \tag{4}$$

In polluted sites, the main idea of Bayesian method for data fusion is to use the Gaussian classifier in the plain Bayesian classifier to input each feature of the samples into the classifier and output the category corresponding to each sample, in order to achieve the purpose of data unification. Sample eigenvalues are mainly obtained by organizing the data from the detailed investigation of the polluted site (e.g., surface coverage, subsurface containment measures, sampling depth, pollutant concentration, etc.), which are classified by the Bayesian method to obtain the category to which the sample belongs.

III. B. XGBoost

XGBoost, also known as Extreme Gradient Boosting Tree, is a further improvement on the gradient boosting algorithm [20]. The XGBoost algorithm uses Newton's method in solving the loss function by Taylor expanding the loss function to the second order and adding L1 and L2 regularization terms.

The XGBoost model is defined as: in a given dataset including N samples and m feature variables $D = \{x_i, y_i\} (\mid D \mid = N, x_i \in R_m, y_i \in R)$, and the predicted output of its integrated model can be expressed as:

$$\overline{y}_i = \phi(x_i) = \sum_{k=1}^{K} f_k(x_i) \tag{5}$$

where f_k is denoted as the regression tree and K is the number of regression trees. When the XGBoost model gets an input x_i, its output value is the sum of the predicted values of K regression trees.

The objective function at the t th moment of XGBoost is defined as:

$$L^{(t)} = \sum_i l(y_i, y_i^{(t-1)} + f_t(x_i)) + \sum_{i=1}^{t} \Omega(f_i) \tag{6}$$

$$\sum_{i=1}^{t} \Omega(f_i) = \Omega(f_t) + C \tag{7}$$

In the above equation, l is the loss function indicating the deviation of the predicted value from the true value, which is generally a convex function, $f_i(x_i)$ is the predicted value of the t th decision tree for the sample i, and $\sum_{i=1}^{t} \Omega(f_i)$ is the sum of complexity of all t threes and it can effectively reduce the complexity of the model and prevent overfitting.

According to the second-order form of Taylor's expansion, the following formula is obtained by second-order expansion of the objective function l at the moment t:

$$L^{(t)} \cong \sum_{i=1}^{N}\left[l(y_i, \hat{y}_i^{(t-1)}) + g_i f_t(x_i) + \frac{1}{2} h_i f_t^2(x_i) \right] + \Omega(f_t) + C \tag{8}$$

where g_i is the first order derivative and h_i is the second order derivative:

$$g_i = \partial_{\hat{y}(t-1)} l(y_i, \hat{y}_i^{(t-1)}) \tag{9}$$

$$h_i = \partial^2_{\hat{y}(t-1)} l(y_i, \hat{y}_i^{(t-1)}) \tag{10}$$

At this point, $l(y_i, \hat{y}_i^{(t-1)})$ is the difference between all the previous trees and is a constant that has no effect on the optimization of the function. Therefore, removing all constant terms, the objective function is obtained as:

$$L^{(t)} \cong \sum_{i=1}^{N}\left[g_i f_t(x_i) + \frac{1}{2} h_i f_t^2(x_i) \right] + \Omega(f_t) \tag{11}$$

The complexity Ω of the tree consists of the number of leaves T and the regular term of the objective function can be expressed as:

$$\Omega(f_t) = \gamma T + \frac{1}{2}\lambda \sum_{j=1}^{T} \omega_j^2 \tag{12}$$

Then, all the samples x_i of the j th leaf node are delimited into a collection of samples I_j of a leaf node, according to the sample-to-leaf node mapping relation q:

$$f_t(x) = \omega_q(x) \tag{13}$$

where ω is the weight of the leaf node. At this point, the objective function can be expressed as:

$$\begin{aligned} L^{(t)} &\cong \sum_{i=1}^{N}\left[g_i \omega_q(x_i) + \frac{1}{2} h_i \omega_q^2(x_i) \right] + \Omega(f_t) \\ &= \sum_{i=1}^{N}\left[g_i \omega_q(x_i) + \frac{1}{2} h_i \omega_q^2(x_i) \right] + \gamma T + \frac{1}{2}\lambda \sum_{j=1}^{T} \omega_j^2 \\ &= \sum_{j=1}^{T}\left[\left(\sum_{ieI_j} g_i \right)\omega_j + \frac{1}{2}\left(\sum_{ieI_j} h_i + \lambda \right)\omega_j^2 \right] + \gamma T \end{aligned} \tag{14}$$

To simplify the expression, define $G_j = \sum_i e_{I_j} g_i$ and $H_j = \Sigma_i e_{I_j} h_i$ to denote the cumulative sum of first-order partial derivatives of all samples at leaf node i and the sum of second-order partial derivatives of all samples at leaf node j, respectively. Then the final objective function is simplified as:

$$L^{(t)} = \sum_{j=1}^{T}\left[G_i \omega_j + \frac{1}{2}(H_j + \lambda)\omega_j^2 \right] + \gamma T \tag{15}$$

The weight ω of leaf node j is solved as $\omega_j^* = -\frac{G_i}{H_i + \lambda}$ using the quadratic quadratic function solution formula. So the objective function is updated as:

$$L^{(t)} = -\frac{1}{2}\sum_{j=1}^{T}\left[\frac{G_j^2}{H_j + \lambda} \right] + \gamma T \tag{16}$$

XGBoost model training speed is faster, the advantages are obvious: in the processing of the loss function using Taylor's second-order expansion, which improves the error accuracy at the same time is conducive to the gradient descent process faster and more accurate, adding regularization, reduces the variance of the model, effectively preventing the model from overfitting, and support for column sampling can reduce the computation and reduce

overfitting. However, the XGBoost model occupies a large amount of memory and takes a long time when the data volume is large.

III. C. Analysis of polybrominated diphenyl ethers and new brominated flame retardants

III. C. 1) PBDES Analysis

The analyzing instrument was GC/MSD (Agilent, 7890/5975C) with NCI source and selective ion scanning mode (SIM). A total of 45 monomers of mono- and nonabromodiphenyl ethers of PBDEs congeners (except BDE-209) were separated and determined on a column (DB-XLB, 30 m×0.25 mm×0.25 μm). Temperature increase program: 110 ℃ (1 min) 8 ℃-min-1→180 ℃ (1 min) 2 ℃-min-1→240 ℃ (5 min) 2 ℃-min -1→280 ℃(2 min)10 ℃ -min-1→310 ℃(35 min). The temperature of the injection port was 260 ℃ and the temperature of the ion source was 250 ℃. The determination of decabromodiphenyl ether (BDE-209) was carried out on a column (DB-5HT, 15 m×0.25 mm×0.1 μm) with the following heating program: 110 ℃ (2 min) 15 ℃-min-1→320 ℃ (2 min) 10 ℃ -min-1→340 ℃ (5 min), 10 ℃-min-1→280 ℃ (2 min) 10 ℃-min-1→310 ℃ (35 min). The heating program was 110 ℃ (2 min) 15 ℃-min-1→320 ℃ (2 min) 10 ℃-min-1→340 ℃ (5 min), the inlet temperature was 260 ℃, and the temperature of ion source was 250 ℃.

The 46 PBDEs monomers analyzed were: decabromodiphenyl ether (Deca-BDEs: BDE-209), nonabromodiphenyl ether (Nona-BDEs: BDE-208), octabromodiphenyl ether (Octa-BDEs: BDE-204, -203,-198, -197, -196), heptabromodiphenyl ether (Hepta-BDEs:BDE -190, -183, -181), hexabromodiphenyl ethers (Hexa-BDEs: BDE-166, -155, -154, -153, -138), pentabromodiphenyl ethers (Penta-BDEs: BDE-126, -119, -118, -116, -100, -99,-85), tetrabromodiphenyl ethers (Tetra-BDEs: BDE-77), and hexabromodiphenyl ethers (Hepta-BDEs: BDE-120, -203, -198, -197, -196). BDEs: BDE-77, -75, -66,-47, -49+71), tribromodiphenyl ethers (Tri-BDEs: BDE-37, -35,-33, -32, -30, -28, -25, -17), dibromodiphenyl ethers (Di-BDEs: BDE-15, -13, -12, -11, -10, -8, -7) and mono-bromodiphenyl ethers (Mono-BDEs: BDE-15, -12, -11, -10, -8, -7). BDEs (Di-BDEs: BDE-15, -13, -12, -11, -10, -8, -7) and Mono-BDEs (Mono-BDEs: BDE-3, -2, -1).

III. C. 2) New Brominated Flame Retardants (NBFRS)

In the 21st century, with the development of new industries and changes in people's lifestyles, some new types of pollutants have emerged: brominated flame retardants such as polybrominated diphenyl ethers (PBDES), pharmaceuticals (including various types of veterinary medicines and antibiotics) and personal care products (PPCPs/PCPS), ammonium perfluorozincate (PFZ), and pollutants of the aromatic sulfonate group (PFOS/PFOA), and phytotoxic substances. These pollutants are new to the environment and are generally found in low concentrations in the environment, but with high ecosystem hazards and human health impacts. Most of the brominated flame retardants have been reported to be highly persistent in the soil environment, capable of accumulating in the human body through the food chain and other pathways, impeding the development of the brain and skeleton through prolonged exposure, and possibly carcinogenic.

Among the five brominated flame retardants, TBBPA is the most widely used and widely produced, with an annual output of about 120,000 tons. It is mainly used as a reactive flame retardant for the flame retardancy of printed wiring boards and the production of brominated epoxy intermediates and brominated polycarbonate, but it is also used as an additive flame retardant for the flame retardancy of ABS, HIPS, epoxy resins, phenolic resins, and unsaturated polyoxides, etc. Although TBBPA has a covalent binding capacity, it can accumulate in the body through other channels. Although TBBPA has covalent binding properties, studies have confirmed that both reactive and additive products release TBBPA and its metabolites into the environment.

IV. Pollution characterization of polybrominated diphenyl ethers and new brominated flame retardants

IV. A. Sample collection of PBDEs and new brominated flame retardants

The linear weighting method was used to obtain the pollution eigenvalues of the samples to quantitatively assess the comprehensive pollution of copper laminates by associating Park's Bayes and XGBoost algorithms, obtaining the characteristic importance of the pollution severity caused by each indicator in each sample and using this as the weight of each indicator.

The detailed information of BPs and BFRs determined in this analysis is shown in Table 1. 12 kinds of BPs single-label and 8 kinds of PBDEs mixed-label were purchased from AccuStandard Company in the U.S.A., and 13 kinds of NBFRs single-label were purchased from Alta Scientific Company in Tianjin, China. BPS), C12-bisphenol AF (C12-BPAF)] and BFRs internal standard [2,3′,4,4′,5-pentabromodiphenyl ether (BDE118), 1,2,3-tribromo-4-(2,3,4-tribromophenoxy)benzene (BDE128)] were purchased from Cambridge Isotope Laboratorie, USA.

Table 1: Basic information of the target compounds

/	Chinese full name	For short	CAS	The water distribution coefficient of the octanolLogKow1	Parent ion mass (m/z)	Subionic mass (m/z)	Collision voltage /eV
Bisphenol compounds (BPs)	Bisphenol A	BPA	80-05-7	3.648	228	134	-26
	Bisphenol B	BPB	77-40-7	4.185	240	210	-26
	4,4'- vinylene Bisphenol	BPE	2081-08-5	3.198	212	199	-26
	Bisphenol F	BPF	620-92-8	2.785	200	100	-26
	Bisphenol P	BPP	2167-51-3	6.158	348	135	-69
	Bisphenol S	BPS	80-09-1	2.164	250	93	-56
	Bisphenol Z	BPZ	843-55-0	5.798	268	150	-56
	Bisphenol AF	BPAF	1478-61-1	3.984	337	263	-38
	Bisphenol AP	BPAP	1571-75-1	4.348	290	275	-30
	Bisphenol BP	BPBP	1844-01-5	5.626	350	275	-20
	Bisphenol M	BPM	13595-25-0	-2	365	135	-38
	Bisphenol G	BPG	127-54-8	6.348	310	300	-38
Polybrominated diphenyl ether(PBDEs)	2,4,4′ - Tribromodiphenyl ether	BDE28	41318-75-6	5.848	-	80(82)	-
	2,2′ ,4,4′ - Tetrabromobenzyl ether	BDE47	5436-43-1	6.788	-	80(82)	-
	2,2′ ,4,4′ ,5-Pentabromodiphenyl ether	BDE99	60348-60-9	6.869	-	80(82)	-
	2,2′ ,4,4′ ,6-Pentabromodiphenyl ether	BDE100	189084-64-8	6.565	-	80(82)	-
	2,2,4,4,5,5-Hexabromodiphenyl ether	BDE153	68631-49-2	7.165	-	80(82)	-
	2,2′ ,4,4′ ,5,6′ -Hexabromodiphenyl ether	BDE154	207122-15-4	7.348	-	80(82)	-
	2,2′ ,3,4,4′ ,5,6-Heptabromodiphenyl ether	BDE183	207122-16-5	7.134	-	80(82)	-
	Decabromodiphenyl ether	BDE209	1163-19-5	12.488	-	490(488)	-
New brominated flame retardant(NBFRs)	2,4,6- Tribromophenyl allyl ether	ATE	3278-89-5	-	-	80(82)	-
	1,2- Dibromine -4-(1,2-Mono-dibromoethyl) Cyclohexane	TBECH	3322-93-8	5.248	-	80(82)	-
	1,2,5,6- Tetrabromocycloctane	TBCO	3194-57-8	5.248	-	80(82)	-
	2,3,4,5,6-Pentabromoethylbenzene	PBEB	99717-56-3	7.487	-	80(82)	-
	2- Bromoallyl -2,4,6-Tribromophenyl ether	BATE	85-22-3	-	-	80(82)	-
	Hexabromobenzene	HBB	87-82-1	7.348	-	80(82)	-
	(2,3- Dibromopropyl) (2,4,6-Tribromophenyl)ether	DPTE	35109-60-5	6.348	-	80(82)	-
	1,2,3,4,5-Pentabromobenzene	PBBZ	23488-38-2	6.464	-	80(82)	-
	2,3,5,6- Tetrabromop-xylene	p-TBX	87-83-2	6.648	-	80(82)	-
	Pentabromotoluene	PBT	608-90-2	6.987	-	80(82)	-
	Hexachlorodibromooctane	HCDBCO	51936-55-1	7.948	-	80(82)	-
	1, 2-bis (2,4, 6-tribromophenoxy) ethane	BTBPE	37853-59-1	9.148	-	80(82)	-
	Tetrabromoo-chlorotoluene	TBCT	39569-21-6	7.384	-	80(82)	-

The organic reagents used in the experiments: dichloromethane, methanol, hexane, acetone, iso-octane, formic acid, acetonitrile, toluene, and ethyl acetate were all chromatographically pure and purchased from Shanghai Amperexperiment Technology Co. Ethylenediamine-N-propylsilylated silica adsorbent (PSA), anhydrous sodium sulfate (⩾99%), disodium ethylenediaminetetraacetic acid (Na2EDTA, ⩾99%), sodium citrate (⩾99%), sodium

chloride (⩾99%), and reversed-phase silica chromatography packing C18 were purchased from Guangzhou Ruixin Biochemistry and Technology Co.

The parent ion mass-to-charge ratios, daughter ion mass-to-charge ratios, and collision voltages of bisphenolic compounds (BPs) ranged from [200,365], [93,300], [-69,-20], and among the polybrominated diphenyl ethers (PBDEs) and new brominated flame retardants (NBFRs), except for decabromodiphenyl ether (DBDE) with a daughter ion mass-to-charge ratio of 490 (488), the daughter ion mass-to-charge ratio for the other ones were all 80 (82).

IV. B. Pollution characterization of PBDEs

IV. B. 1) Concentration distribution of PBDEs

The monitoring results of PBDEs in sorting residues of copper laminates are shown in Table 2.The PBDEs monomer with the highest detection frequency in the nine sampling points of copper laminates was BDE99, which was detected in all the monitoring points, followed by BDE47 and BDE153, and BDE154, BDE183, and BDE209 were not detected in all the monitoring points.The concentration of BDE99 was 0.158~0.498ng/L, and the concentration of pollutants detected in June and October was 1.088 ng/L, 1.657 ng/L, respectively. 0.498 ng/L, copper laminate sorting residue H1 point has the highest concentration, June and October detected pollutant concentration of 1.088 ng / L, 1.657 ng / L. BDE47 detected concentration in the range of 0.158~0.549 ng / L, is also the highest concentration of H1 point. The range of ΣPBDEs in the copper laminate residue was 0.158~1.657ng/L, the highest concentration at point H1 was 1.657 ng/L, followed by point H3 of the copper laminate with a concentration of 1.115 ng/L, and the lowest detected concentration was at point H7 of the copper laminate, with a concentration of 0.158 ng/L. From the above data, it can be seen that there is a higher concentration of PBDEs aggregated at the inlet. The concentrations at points H5, H6 and H7 in the east copper laminate were significantly lower than those at points H1, H2, H3 and H4 in the west copper laminate.ΣThe concentration of PBDEs in October was greater than that in June, which may be related to the fact that June is the season with the most precipitation of the year in the country. The main PBDEs detected in the copper laminates were BDE47 and BDE99, which were also the most highly detected monomers in other copper laminates around the world. The results of the study were in general agreement with the level of PBDEs contamination in the sorting residues of the copper laminates.

Table 2: The concentration of PBDEs in the residue of copper laminate(ng/L)

Compound	Time	H1	H2	H3	H4	H5	H6	H7	H8	H9
BDE28	June	0.156	ND	ND	ND	ND	ND	ND	ND	ND
	October	0.164	ND	ND	ND	ND	ND	ND	ND	ND
BDE47	June	0.348	0.348	0.125	0.136	ND	ND	ND	0.198	0.248
	October	0.549	0.364	0.269	0.284	ND	ND	ND	0.428	0.462
BDE99	June	0.436	0.248	0.214	0.175	0.248	0.234	0.158	0.406	0.248
	October	0.487	0.324	0.498	0.396	0.279	0.289	0.289	0.459	0.348
BDE100	June	ND	ND	ND	ND	ND	ND	ND	ND	ND
	October	0.159	ND	ND	ND	ND	ND	ND	ND	ND
BDE153	June	0.148	0.105	0.125	ND	ND	ND	ND	ND	0.125
	October	0.298	ND	0.348	ND	ND	ND	ND	ND	0.264
BDE154	June	ND	ND	ND	ND	ND	ND	ND	ND	ND
	October	ND	ND	ND	ND	ND	ND	ND	ND	ND
BDE183	June	ND	ND	ND	ND	ND	ND	ND	ND	ND
	October	ND	ND	ND	ND	ND	ND	ND	ND	ND
BDE209	June	ND	ND	ND	ND	ND	ND	ND	ND	ND
	October	ND	ND	ND	ND	ND	ND	ND	ND	ND
∑PBDEs	June	1.088	0.701	0.464	0.311	0.248	0.234	0.158	0.604	0.621
	October	1.657	0.688	1.115	0.68	0.279	0.289	0.289	0.887	1.074

IV. B. 2) Production potential

The above results show that the hydrogen supply capacity of the copper laminate is extremely weak, and once the PBDEs are photolysed in water to generate neighboring bromine radicals, there is a risk that most of them will be converted to PBDFs. lg(R/RBDE-1) is calculated as shown in Fig. 3, and different structures show different potentials for the generation of PBDFs, with negative values indicating that the potential for the generation of

PBDFs is greater than that of BDE1, and positive values are less than that of BDE1, the smaller the values, the greater the potential for the generation of PBDFs. BDE1, the smaller the value, the larger the PBDFs generation potential, when the Br position at 2',3',4',5',6', the value is -2.848, indicating that the PBDFs generation potential is the largest.Structures with PBDFs generation potentials smaller than BDE1 almost always contain at least three neighboring bromines, because the rate constants for the cycloadditions of the carbons substituted by free radical attacking the neighboring bromines are low. Although the calculations show little difference in the cyclization ratios of different PBDEs in the copper laminate sorting residue due to the very weak hydrogen supply capacity of the copper laminate, the difference in lg(R/RBDE-1) is more pronounced, and thus this parameter can be used as a reference to assess the potential of PBDEs for generating PBDFs when they are in other hydrogen supplying media.

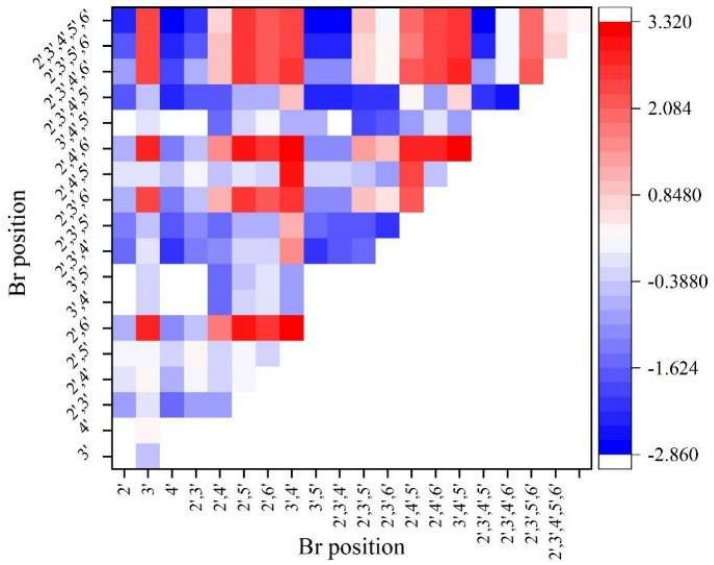

Figure 3: The relative PBDFs formation potential of PBDEs compared with BDE1

IV. B. 3) Statistics of PBDEs in residues

Table 3 shows the levels of PBDEs congeners and Σ8 PBDEs. Among the eight PBDEs monomers tested, the detection rates of BDE47, BDE99, BDE100 and BDE209 were all 100%, while the detection rates of BDE28, BDE153, BDE154 and BDE183 were 85%, 98%, 90% and 79%, respectively, which were also above 78%, which indicated that PBDEs have been the residues of copper laminate sorting The contents of Σ7PBDEs ranged from 9.166 to 88.326 ng·g-1, with median and mean values of 29.092 ng·g-1 and 34.377 ng·g-1, respectively.

Table 3: PBDEs isophysical and the level of Σ8PBDEs

Item	Median(ng·g^{-1})	Mean(ng·g^{-1})	SD(ng·g^{-1})	Min(ng·g^{-1})	Max(ng·g^{-1})	Detection rate/%
BDE28	1.648	2.549	2.248	ND	8.825	85
BDE47	8.485	9.785	5.358	2.545	21.266	100
BDE99	8.648	9.845	5.596	2.569	22.236	100
BDE100	3.215	3.945	2.655	4.052	10.296	100
BDE153	2.596	3.048	2.152	ND	8.623	98
BDE154	2.015	2.569	2.148	ND	8.515	90
BDE183	2.485	2.636	2.266	ND	8.565	79
Σ7PBDEs	29.092	34.377	22.423	9.166	88.326	100
BDE209	47.483	64.488	53.788	8.266	292.265	100
Σ8PBDEs	76.575	98.865	76.211	17.432	380.591	100

IV. C. Pollution characteristics of new brominated flame retardants

IV. C. 1) Mass concentrations of BPs, BFRs in sediments

Table 4 shows the mass concentrations of BPs and BFRs in the residues. 5 BPs were detected in the copper laminate deposits, among which the detection rates of BPA, BPB, and BPAF were >50%, which were 84.648%, 61.548%, and 61.548%, respectively. The total mass concentration of BPs was <LOD-44.021 ng·g−1 (median

7.684 ng·g−1). Referring to the studies of other scholars, the mass concentrations of BPs in the residues of copper laminates were 3.92-151 ng·g−1 before sorting and 2.16-59.0 g·g−1 after sorting, which were higher than the residues in this study, and the present concentration was higher. After the sorting operation of copper laminates, BPs were easy to enter the water body and enriched in the residue, while after the long-term protection and treatment work, all kinds of pollution sources around the Taihu Lake Basin were more strictly controlled, which made the concentration of BPs in the residue at a lower level.

Table 4: The quality of BPs, BFRs in the residue

Compound	Residual concentration of medium matter/(ng·g^{-1})		
	Detection rate /%	Median	Range
BPA	84.648	3.245	<LOD-4.488
BPB	61.548	4.415	<LOD-12.896
BPE	46.236	<LOD	<LOD-25.783
BPS	15.485	<LOD	<LOD-0.136
BPAF	61.548	0.024	<LOD-0.718
∑BPs	/	7.684	<LOD-44.021
BDE28	15.469	<LOD	<LOD-0.478
BDE47	61.536	0.245	<LOD-2.299
BDE99	100	0.655	0.306-2.756
BDE153	100	0.096	0.029-0.971
BDE183	53.845	0.248	<LOD -1.415
BDE209	100	0.398	0.086-10.455
∑PBDEs	/	1.642	0.421-18.374
TBCT	38.569	<LOD	<LOD-0.053
PBT	23.133	<LOD	<LOD-0.615
DPTE	30.946	<LOD	<LOD-0.752
HBB	38.569	<LOD	<LOD-0.766
HCDBCO	7.748	<LOD	<LOD-1.548
∑NBFRs	/	/	<LOD-3.734

IV. C. 2) Correlation analysis between different pollutants in residues

Spearman rank correlation analysis was performed for compounds with ⩾50% detection rate in the sediments, and the results of Spearman rank correlation analysis between different contaminants in the residues are shown in Fig. 4. There was a significant positive correlation between BPA and BPAF (r=0.54, p=0.048<0.05), which suggests that BPA and BPAF may share the same source of contamination, such as copper laminate sorting residues.

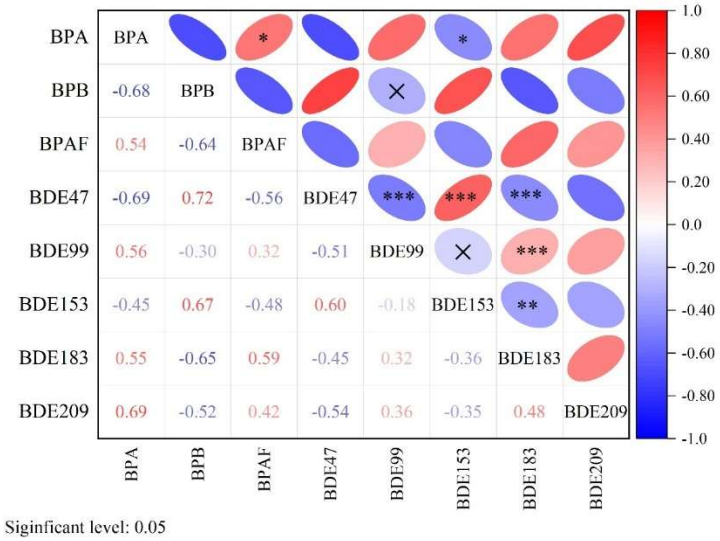

Figure 4: The spearman rank correlation analysis between different pollutants in the residue

*:p≤0.05,**:≤0.01,***:p≤0.001.

IV. C. 3) Temporal Trends in Substitution of NBFRs

The ratio of Σ26PBDEs to Σ5NBFRs was used to initially determine the substitution of new brominated flame retardants over time. Figure 5 shows the temporal trend of the ratio of traditional and new brominated flame retardants. Σ26PBDEs and Σ5NBFRs are shown in Figure 5. (a) is the ratio of Σ26PBDEs to Σ5NBFRs, (b) is the ratio of decabromodiphenyl ether (DDE) and its alternatives, (c) is the ratio of octabromodiphenyl ether (OBE) and its alternatives, and (d) is the ratio of pentabromodiphenyl ether (PentaBDE) and its alternatives. Σ26PBDE/Σ5NBFRs show a generally decreasing trend The average value of Σ26PBDE/Σ5NBFR was 4.233 in 2011, which was significantly higher than that of 2.302 in 2013 and 2.073 in 2021 ($p<0.01$), indicating that the newer brominated flame retardants are gradually replacing the traditional brominated flame retardants. The ratios of penta-, octa- and decaBDE and their alternatives (BDE47,99,100)/(TBB,TBPH), (BDE154,153,183)/ BTBPE, BDE209/DBDPE were further analyzed separately. The ratios of decabromodiphenyl ether and its alternatives showed a decreasing trend over time, with one-way ANOVA results indicating that the ratio in 2011 was significantly higher than that in 2013 and 2021 (both $p < 0.05$). No significant differences in the ratios of octa- and pentaBDE to their alternatives were observed between years. The small change in the ratio of octaBDE and its alternatives over time could be attributed to the fact that octaBDE is produced and used in a small amount in China, and therefore its change is less fluctuating. The ratio of PentaBDE and its alternatives increased between 2016 and 2021, mainly due to the increase in the monomer content of PentaBDE, which, combined with the previous analysis, is presumed to come from the debromination degradation of BDE209 and other highly brominated congeners.

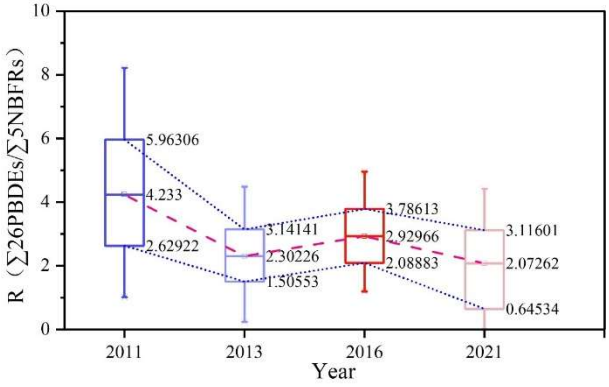

(a) The ratio of Σ26PBDEs and Σ5NBFRs

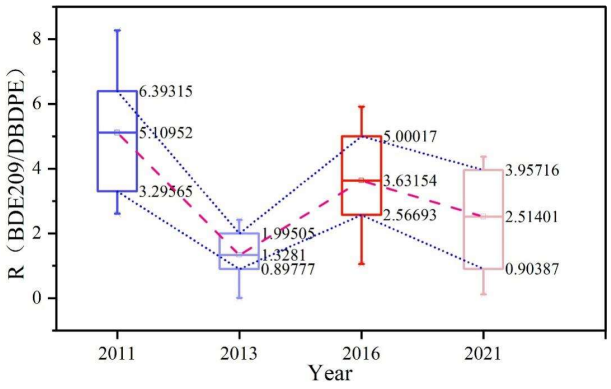

(b) BDE209/DBDPE

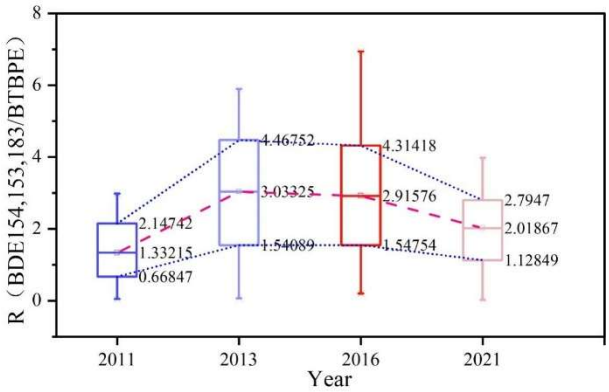

(c) BDE154,153,183/BTBPE

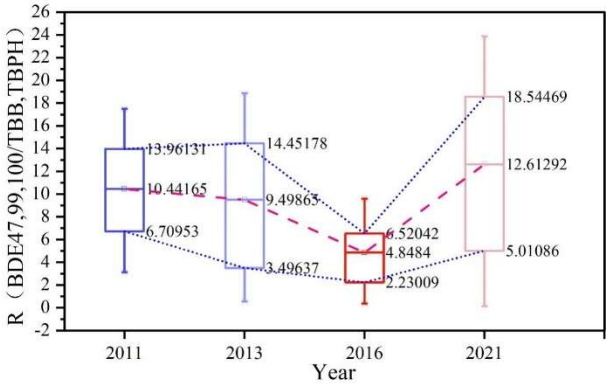

(d) (BDE47,99,100)/(TBB,TBPH)

Figure 5: The time of the traditional and new brominated flame retardant content ratio

V. Conclusion

The contamination characteristics of PBDEs and new brominated flame retardants (BFRs) in the sorting residues of copper laminates were successfully identified based on the associative analysis of the plain Bayes and XGBoost algorithms. The spatial distribution of the contaminants showed obvious regional differences, and the contamination concentrations at the western measuring points H1, H2, H3 and H4 were significantly higher than those at the eastern measuring points H5, H6 and H7, among which the concentration of ΣPBDEs at point H1 reached 1.657 ng/L, which was the highest among all the measuring points.The detection patterns of the eight PBDEs singles were significantly different, and the detection rates of BDE47, BDE99, BDE100 and BDE209 were all detected at 100%, indicating that these compounds have become the main pollutants in the residues, while BDE154 and BDE183 were not detected in all the monitoring points, reflecting the differences in the environmental behaviors of different brominated number compounds. The substitution process of new brominated flame retardants is obvious, with the ratio of Σ26PBDEs/Σ5NBFRs decreasing continuously from 4.233 in 2011 to 2.073 in 2021, and the substitution of decabromodiphenyl ether is the most significant, with the ratio of BDE209/DBDPE in 2011 significantly higher than that in 2013 and 2021. The machine learning method effectively reveals the main controlling factors of the pollution features, the XGBoost algorithm provides a quantitative basis for weight setting by evaluating the importance of the features, and the results of the plain Bayesian classification are highly consistent with the actual pollution level. Correlation analysis revealed a significant positive correlation between BPA and BPAF, indicating that they may have the same pollution source. These results provide an important reference for the development of targeted pollution management strategies and demonstrate the value of machine learning in environmental pollution characterization.

Acknowledgement

The author thanks the National Special Fund for the Prevention and Control of Heavy Metal Pollution for its funding: Phase II of the Heavy Metal Pollution Control Project for the Dismantling Industry of Waste Electrical and Electronic Products in Qingyuan City.

Funding

This work was supported by Project Phase II of the Heavy Metal Pollution Control of WEEE Dismantling Industry Program in Qingyuan.

Data available with the paper

The author declares that data supporting the results of this study can be obtained in the paper. If readers need raw data files in other formats, they can request them from the corresponding authors. The original data are provided together with this article.

Conflict of Interest

The author declares that they have no conflict of interest.

References

[1] Weber, R., Herold, C., Hollert, H., Kamphues, J., Ungemach, L., Blepp, M., & Ballschmiter, K. (2018). Life cycle of PCBs and contamination of the environment and of food products from animal origin. Environmental Science and Pollution Research, 25, 16325-16343.

[2] Zhu, M., Yuan, Y., Yin, H., Guo, Z., Wei, X., Qi, X., ... & Dang, Z. (2022). Environmental contamination and human exposure of polychlorinated biphenyls (PCBs) in China: A review. Science of the Total Environment, 805, 150270.

[3] Liu, X., Fiedler, H., Gong, W., Wang, B., & Yu, G. (2018). Potential sources of unintentionally produced PCB, HCB, and PeCBz in China: A preliminary overview. Frontiers of Environmental Science & Engineering, 12, 1-14.

[4] Conseil, H., Stendahl Jellesen, M., & Ambat, R. (2014). Contamination profile on typical printed circuit board assemblies vs soldering process. Soldering & Surface Mount Technology, 26(4), 194-202.

[5] Güzel, B., Canlı, O., & Çelebi, A. (2022). Characterization, source and risk assessments of sediment contaminants (PCDD/Fs, DL-PCBs, PAHs, PCBs, OCPs, metals) in the urban water supply area. Applied Geochemistry, 143, 105394.

[6] Reddy, A. V. B., Moniruzzaman, M., & Aminabhavi, T. M. (2019). Polychlorinated biphenyls (PCBs) in the environment: Recent updates on sampling, pretreatment, cleanup technologies and their analysis. Chemical Engineering Journal, 358, 1186-1207.

[7] Mastin, J., Harner, T., Schuster, J. K., & South, L. (2022). A review of PCB-11 and other unintentionally produced PCB congeners in outdoor air. Atmospheric Pollution Research, 13(4), 101364.

[8] Yu, D., Duan, H., Song, Q., Liu, Y., Li, Y., Li, J., ... & Wang, J. (2017). Characterization of brominated flame retardants from e-waste components in China. Waste Management, 68, 498-507.

[9] Boro, B., & Tiwari, P. (2024). Effect of metals and brominated flame retardants on thermal degradation kinetics of waste printed circuit board. Thermochimica Acta, 736, 179747.

[10] Wang, R., Zhu, Z., Tan, S., Guo, J., & Xu, Z. (2020). Mechanochemical degradation of brominated flame retardants in waste printed circuit boards by Ball Milling. Journal of hazardous materials, 385, 121509.

[11] Ike-Eze, I. C. E., Ucheji, O. N., Ubi, P. A., Oji, E. O., Aigbodion, V. S., Omah, A. D., & Ogbuefi, C. C. (2023). An Overview of Flame Retardants in Printed Circuit Boards for LEDs and other Electronic Devices. J. Mater. Environ. Sci., 14 (4), 410, 420.
[12] Tan, Q., Liu, L., Yu, M., & Li, J. (2020). An innovative method of recycling metals in printed circuit board (PCB) using solutions from PCB production. Journal of Hazardous Materials, 390, 121892.
[13] Ning, C., Lin, C. S. K., Hui, D. C. W., & McKay, G. (2018). Waste printed circuit board (PCB) recycling techniques. Chemistry and Chemical Technologies in Waste Valorization, 21-56.
[14] Oke, E. A., & Potgieter, H. (2024). Discarded e-waste/printed circuit boards: a review of their recent methods of disassembly, sorting and environmental implications. Journal of Material Cycles and Waste Management, 26(3), 1277-1293.
[15] Altarawneh, M., Saeed, A., Al-Harahsheh, M., & Dlugogorski, B. Z. (2019). Thermal decomposition of brominated flame retardants (BFRs): Products and mechanisms. Progress in Energy and Combustion Science, 70, 212-259.
[16] MajidPakizeh & RasoulRahimnia. (2024). Water desalination using CaCO3/blend of polyphenylene oxide and polystyrene mixed matrix membranes in a direct contact membrane distillation (DCMD) unit. Polymer Engineering & Science,65(3),1106-1122.
[17] Nattha Ingavat,Xinhui Wang,Yee Jiun Kok,Nuruljannah Dzulkiflie,Han Ping Loh,Eunice Leong... & Wei Zhang. (2025). Affinity resin selection for efficient capture of bispecific antibodies as guided by domain composition. Process Biochemistry,154,1-11.
[18] LiangliangRen & DeyuanZhang. (2025). Mechanical Properties and Failure Mechanisms of Carbon Fiber/Resin Composites with Hot Press, Single‐Vacuum‐Bag, and Double‐Vacuum‐Bag Processes. Advanced Engineering Materials,27(7),2402136-2402136.
[19] Xiaoliang Zhou,Yongli Wang,Li Zhang,Anqi Huang & Xiaoli Wang. (2025). An innovative multi-view collaborative optimization framework for Weighted Naive Bayes. Knowledge-Based Systems,317,113378-113378.
[20] Yanqi Wu,Daqing Cai,Sheng Gu,Nan Jiang & Shengli Li. (2025). Compressive strength prediction of sleeve grouting materials in prefabricated structures using hybrid optimized XGBoost models. Construction and Building Materials,476,141319-141319.